Desalination and Water Treatment
www.deswater.com
doi: 10.1080/19443994.2014.963160

56 (2015) 1669–1680
November

Taylor & Francis
Taylor & Francis Group

Adsorption behavior of fluoride ion on trimetal-oxide adsorbent

Tahir Rafique[a,*], Khalid Mehmood Chadhar[a,b], Tanzil Haider Usmani[a], Saima Qayyum Memon[b], Khaula Shirin[a], Shaikh Kamaluddin[a], Faisal Soomro[c]

[a]*Applied Chemistry Research Center, PCSIR Laboratories Complex, Karachi 75280, Pakistan, Tel. +92 21 34651594; Fax: +92 21 34641847; email: tahirrafique92@yahoo.com (T. Rafique), Tel. +92 333 7123354; emails: khalid.mehmood@pgjdc.org (K.M. Chadhar), usmanith@gmail.com (T.H. Usmani), Tel. +92 333 3109137; emails: khaula_ark@yahoo.com (K. Shirin), shkamaluddin01@hotmail.com (S. Kamaluddin)*
[b]*Institute of Advanced Research Studies in Chemical Sciences, University of Sindh, Jamshoro, Pakistan, email: msaima77@yahoo.co.in (S.Q. Memon)*
[c]*Department of Chemistry, University of Karachi, Karachi, Pakistan, Tel. +92 332 2149007; email: fezzsumro@yahoo.com (F. Soomro)*

Received 4 April 2014; Accepted 17 July 2014

ABSTRACT

The suitability of trimetal-oxide (a refractory waste material) as a possible adsorbent has been studied for the removal of fluoride ion from the aqueous solution. Batchwise experiments have been conducted for following the adsorption behavior. The effect of various variables such as shaking time, hydronium ion concentration, initial fluoride concentration, and adsorbent dose were studied. Freundlich, Langmuir, Dubinin–Radushkevich, and Temkin isotherms were applied to calculate the adsorption behavior of fluoride and were found to be in good agreement with the experimental data, and the mechanism was of chemisorption. The kinetics of the adsorption phenomenon was also studied using Lagergren pseudo-first-order, pseudo-second-order and intra-particle diffusion models, and the results showed that the process of the adsorption of fluoride follows pseudo-first-order as well as pseudo-second -order kinetic models. The adsorbent has shown high defluoridation efficiency of 78% between pH 6.0 and 7.0. The trimetal-oxide was characterized by WD-XRF and XRD techniques before adsorption, and the most dominant components were found to be Al_2O_3, CaO, and MgO with diaspore, calcite, and dolomite being the major mineral phases.

Keywords: Fluoride; Thar Desert; Adsorption; Intra-particle diffusion; Chemisorption

1. Introduction

Presence of high fluoride in groundwater is quite a frequent problem and occurs across various areas of Asia, Africa, and North and South American continents [1,2]. Thar Desert, located in the southeastern part of Sindh province, has also been identified as the most fluoride affected area in Pakistan [3–6]. The quality of groundwater in this region depreciates to alarming levels due to high fluoride concentration of 32 mg/L, whereas the maximum contaminant level of fluoride in drinking water as established by the US EPA is 4 mg/L [7], while the guideline value set by the World Health Organization is 1.5 mg/L [8]. The presence of excessive fluoride in the groundwater used for drinking purposes is known to cause various health problems such as dental and skeletal fluorosis (permanent bone and teeth deformities) in humans

*Corresponding author.

and animals. Other skeletal problems linked to fluoride toxicity include stiffness, rheumatism, and permanent crippling rigidity [9], and the occurrence of these diseases are quite common in the areas of Thar Desert [4]. Therefore, it becomes necessary to keep the level of fluoride concentration within the maximum permissible limit.

Recently many methods, such as adsorption [10–13], ion exchange [14], chemical precipitation with calcium and aluminum salts [15,16], electrodialysis [17–19], and membrane filtration [20], have been used to remove excessive fluoride ions from aqueous solution. Adsorption process has been generally found to be more effective and economical at low concentration levels [21]. However, the economics of the process is affected by high cost of adsorbents. So, the adsorbents with low cost and high efficiency are necessary for the removal of fluoride from aqueous solution. Adsorbents, such as montmorillonite [22], Al_2O_3/CNT [23], activated alumina and modified alumina [24–26], fly ash [27], silica gel [28], bone char [29], and zeolite [30], have also been used but their feasibilities have to be established. Apart from these, several nanocomposite, biocomposite materials [31–33] along with mixed oxides [34–37] and organic carbon from different materials [38–41] have also been reported as efficient fluoride adsorbents. Extensive R&D studies are therefore needed to find an ideal adsorbent for fluoride removal which should have uniform accessible pores, high surface area, and physical and chemical stability [42].

During the present work, systematic studies have been planned and executed to investigate trimetal-oxide as an adsorbent for removal of fluoride ions in aqueous solutions. Different variables like initial fluoride concentration, shaking time, adsorbent dosage, and pH have been optimized during the course of these studies. The adsorption mechanism of fluoride ion on the trimetal-oxide adsorbent was also investigated by analyzing adsorption isotherms and kinetics.

2. Materials and methods

2.1. Source and conditioning of the adsorbent

The trimetal-oxide was primarily collected from a local steel mill where it is being used as refractory ceramics and is usually discarded after use and is usually available in appreciable quantity and sold to mineral market as a waste material. Five raw samples of trimetal-oxide (2 kg) were picked up on random basis from big lots of blocks. The samples of blocks were individually processed into finely divided form by first crushing the blocks in a thoroughly cleaned jaw crusher and thereafter mixed and homogenized by steel roller. Finally, the homogenized sample was pulverized in a ball mill and sieved through 250 μm (60 mesh) sieve. The sieved samples were then washed with deionized water and dried at 105°C for 2 h. The finished dried material is then used as the base material in the present studies.

2.2. Reagents

Stock solution of 1,000 mg/L fluoride was prepared in a one liter volumetric flask by dissolving 2.21 g of anhydrous sodium fluoride in deionized water (conductivity < 1 μS/cm). All the standard solutions were prepared by appropriate dilution of the stock solution with deionized water. The pH of deionized water was about 5.8, and all the experiments were conducted at ambient temperature (30 ± 2°C). The pH of the solutions was maintained in the range of 2.0–12.0 for adsorption experiments using 0.1 N HCl and NaOH solutions, respectively, and all the reagents used in this study were of analytical grade.

2.3. Analytical method

Known amount of trimetal-oxide and standard fluoride solution has been taken in a 100 ml conical flask and agitated on an orbital shaker at constant speed for different intervals of time and filtered through Whatman No. 41 filter paper. The fluoride concentration and pH of the filtrate were determined by using Thermo Scientific Orion 5-Star pH/ISE/DO/conductivity meter. Total ionic strength adjustment buffer (TISAB-IV) was prepared by dissolving 58 g of sodium chloride, 57 ml of glacial acetic acid, and 150 ml of 6 M NaOH solution with a little deionized water, and the volume was made up to 1,000 ml [43]. Samples for fluoride analyses have been diluted to 1:1 with TISAB-IV solution in order to maintain the pH of solution at 5.5 and to eliminate the interference of complexing ions. The fluoride ion selective electrode was calibrated prior to each experiment in order to determine the slope and intercept of the electrode and the pH meter was also calibrated at every measurement by using pH calibration buffers.

The amount of fluoride (mg) adsorbed per unit mass of the adsorbent (g) has been calculated from the following equation;

$$q = \frac{(C_0 - C_e) \times V}{m} \quad (1)$$

where q is the amount of fluoride adsorbed (mg/g), C_0 is the initial concentration of fluoride (mg/L), C_e is

the concentration of fluoride (mg/L) in solution at equilibrium time, V is the adsorbate volume (L), and m is the mass of the adsorbent (g).

2.4. Batch adsorption studies

Batchwise adsorption studies have been conducted to study the effect of various parameters on the adsorption efficiency of fluoride onto trimetal-oxide. A known amount of adsorbent was added in a 100 ml Erlenmeyer flask containing 50 ml of the spiked solution of fluoride, and the flasks were kept in an orbital shaker at 100 rpm and 30 ± 2 ℃ (ambient) for specified period of time. The solution was thereafter filtered through No. 41 filter paper and was allowed to settle. Residual fluoride ion concentrations were immediately determined in each of the case. All the experiments were performed in triplicate, and the mean values have been reported. Fluoride adsorption capacity of trimetal-oxide was established by taking 0.5–5.0 g amount of adsorbent shaken with 10 mg/L fluoride solution for 70 min. The variables of initial fluoride concentration and contact time have been optimized by varying fluoride concentrations from 10 to 100 mg/L at constant adsorbent dose of 0.5 g. The effect of pH on the adsorption of fluoride in the case has been studied between 2.0 and 12.0. Residual fluoride concentration in each of the case was determined after attaining adsorption equilibrium.

2.5. Elemental and phase analyses of adsorbent

The elemental analysis of trimetal-oxide adsorbent material has been carried out by the X-ray fluorescence (XRF), spectrophotometer (Brukers AXS S4 Pioneer), and mineralogical characterization by Siemens D5000 powder diffractometer. Data have been collected from 10° to 90° 2θ using a step size of 0.05°/s and phase identification by Diffrac^{pus} searching software version 7.0.108.

3. Results and discussion

3.1. Characterization of adsorbent

3.1.1. XRF studies

The percentage of major elements found in oxide form in trimetal-oxide adsorbent is given in Table 1, and the most dominant components were found to be Al_2O_3 (40.40%), CaO (30.65%), and MgO (22.1%), respectively. The data clearly show that the adsorption capacity increases with the increase in the oxides Al, Ca, and Mg. Fluoride reacts with hydroxyl group present on oxide/hydroxide of these metals, particularly aluminum oxide/hydroxide has greater ion exchange ability. Hence, the amount of fluoride adsorbed onto these oxide/hydroxide increases with increasing equilibrium concentrations. Anion adsorption sites onto these oxides/hydroxides are aqua $(AlOH)^{2+}$ and hydroxy (AlOH) groups, therefore, F^- can be adsorbed by positively charged or neutral surfaces [44].

Table 1
Chemical composition of trimetal-oxide adsorbent using WD-XRF

Elemental composition	Weight %
Al_2O_3	40.40
CaO	30.65
MgO	22.10
SiO_2	2.636
Fe_2O_3	1.534
P_2O_5	0.773
TiO_2	0.631
LOI	1.197

3.1.2. XRD studies

Results of XRD analysis of trimetal-oxide adsorbent with its mineral phases, their formulae, and percent quantities have been given in Table 2. It may be seen that trimetal-oxide is composed of diaspore (43.60%), calcite (30.20%), and dolomite (20.90%) as the dominant phases and it further confirms the absence of impurities and other phases in the material on the 2-Theta-Scale.

3.2. Optimization of adsorption parameters

3.2.1. Equilibrium time

Fig. 1(A) and (B) shows that the equilibrium has been established within 70–80 min time, and these further indicate that the curves are linear, approaching to saturation, suggesting possible monolayer coverage.

Table 2
Qualitative and quantitative mineral identification of trimetal-oxide adsorbent using XRD

Mineral name	Formula	Sequential quantities (%)
Diaspore	$Al_2O_3{\cdot}H_2O$	43.60
Calcite	$CaCO_3$	30.20
Dolomite	$CaMg(CO_3)_2$	20.90

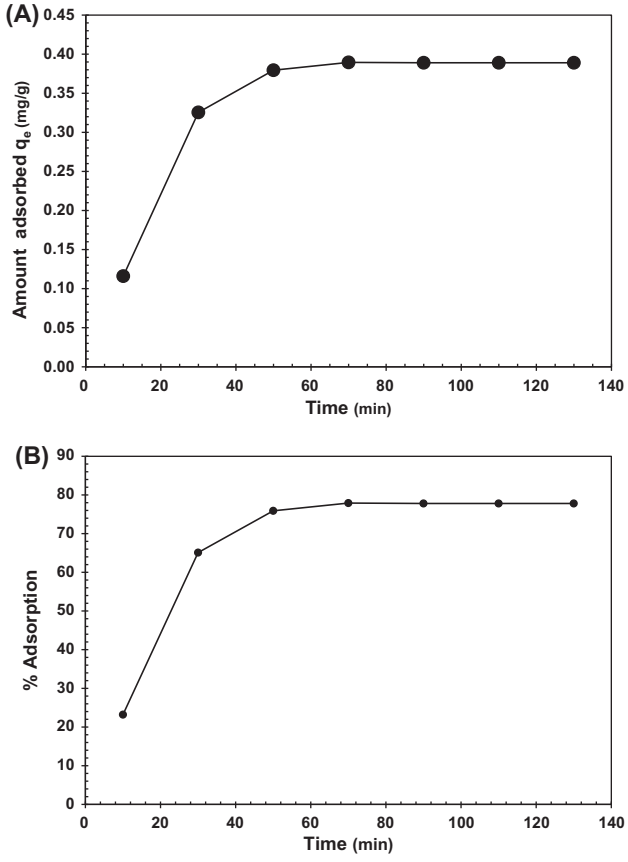

Fig. 1. Effect of equilibrium time on (A) adsorption capacity (B) percentage adsorption, at different initial fluoride concentration (adsorbent dose = 1 g, initial F^- conc. = 10 mg/L, pH = 7, particle size = 250 μm, shaking speed = 100 rpm).

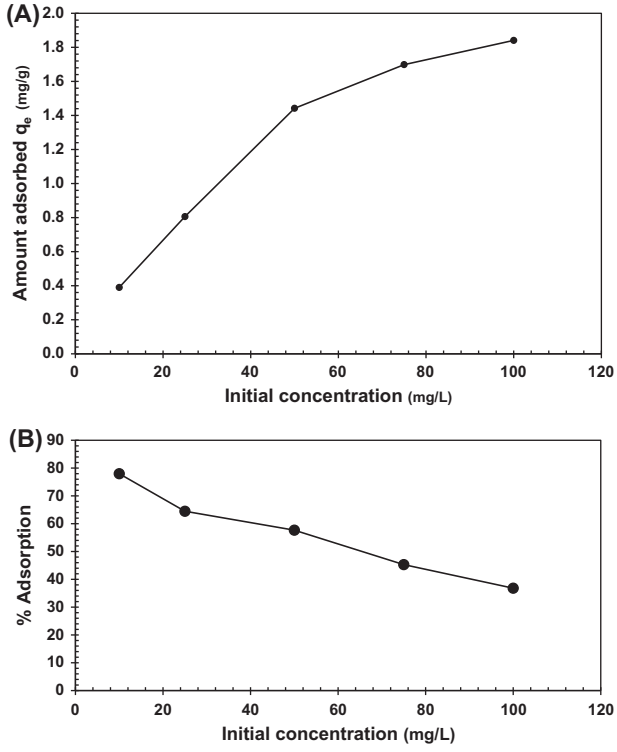

Fig. 2. Plots of (A) amount of fluoride adsorbed per gram of adsorbent and (B) percentage of fluoride adsorption on adsorbent, as a function of initial fluoride concentration (adsorbent dose = 1 g, contact time = 70 min, pH = 7, particle size = 250 μm, shaking speed = 100 rpm).

3.2.2. Effect of initial concentration of adsorbate

It may further be observed in Fig. 2(A) and (B) that the percentage of adsorption decreases with the increase in the initial concentration of fluoride solution, but the actual amount of fluoride adsorbed per unit mass of the adsorbent increases with increase in the fluoride concentration. At lower concentration, the ratio of fluoride ions to the available surface area is low and, therefore, the fractional adsorption becomes independent of initial concentration. However, at higher concentration, the available sites of adsorption become fewer; hence, the percentage removal of fluoride ion decreases with the increase in the initial concentration of fluoride ion in aqueous solution.

3.2.3. Effect of adsorbent dose

In order to investigate the effect of adsorbent dose, different amount of trimetal-oxide was used at constant fluoride concentration of 10 mg/L. The reaction was fast during the first 10 min and equilibrium reached within a period of 80–100 min. Fig. 3(A) shows that with the increase in the dose of adsorbent, the amount of fluoride adsorbed decreases per unit mass of the adsorbent mainly due to the surface coverage. Similarly, Fig. 3(B) shows that the removal efficiency slightly decreases with the increase of the amount of adsorbent as the amount of dose increased. It may be explained by the fact that more the mass of an absorbent is available, greater the surface sites will be available for adsorption. These results have been found qualitatively in good agreement with those found in the literature [45–48]. The best removal efficiency of 78% was obtained with 1.0 g dose of trimetal-oxide.

3.2.4. Effect of pH

Fig. 4(A) and (B) shows that the amount of fluoride adsorbed per gram of adsorbent, and the percentage adsorption of fluoride was optimum and within pH range of 6.0–7.0. Further, the adsorption efficiency decreased with the increase in pH of the solution

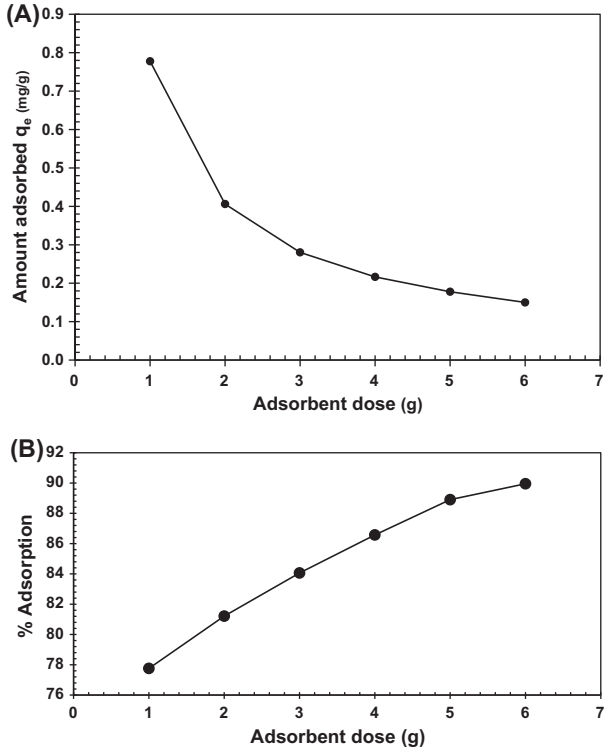

Fig. 3. (A) Effect of adsorption capacity, (B) percentage of adsorption (contact time = 70 min, initial F^- conc. = 10 mg/L pH = 7, particle size = 250 μm, shaking speed = 100 rpm).

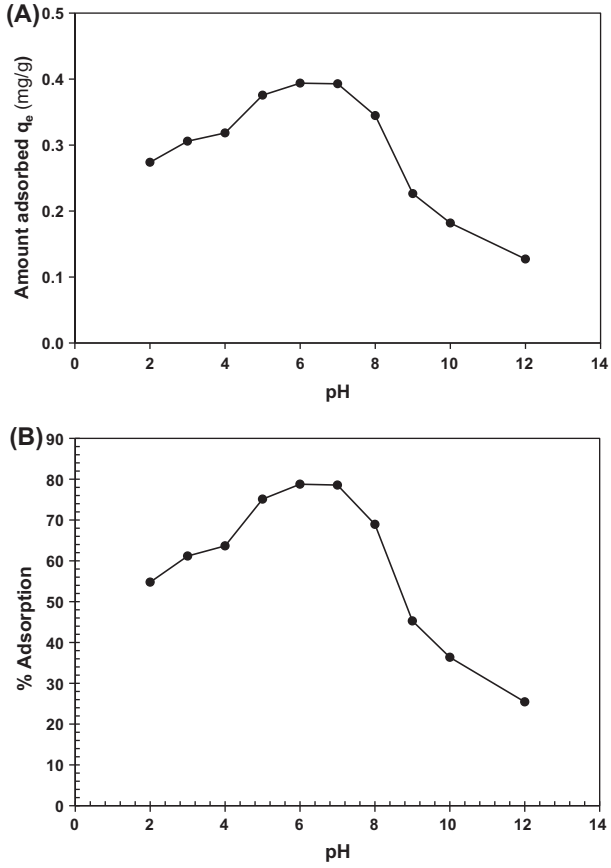

Fig. 4. Effect of pH on (A) fluoride adsorption capacity and (B) the percentage adsorption (adsorbent dose = 1 g, initial F^- conc. = 10 mg/L contact time 70 min, particle size = 250 μm, shaking speed = 100 rpm).

which may be due to the electrostatic repulsion of the fluoride ion to the negatively charged surface and competition for active sites by excess amount of hydroxyl ions. The strong force of interaction between the fluoride ion and the adsorbent plays a significant role, and either H^+ or OH^- ions may influence the adsorption capacity [47], and the interaction is higher at pH > 8.0 due to competition of OH^- ions with fluoride ions for the adsorption sites. At a pH lower than 6, there is greater tendency of F^- to combine with H^+ to form HF^{2-}complex [49] due to the presence of greater number of H^+. Hence, F^- favors to make complex with H^+ rather than being adsorbed on the surface of adsorbent. Therefore, the results showed that the adsorption is lower at lower pH values. However, at a pH range of 6.6–8.0, the concentration of H^+ ions in the solution is approximately equal to the concentration of OH^- ions and, therefore, there is more possibility of F^- to get adsorbed on to the surface.

3.3. Adsorption kinetic models

The data as regards adsorption kinetic is prerequisite while designing batch sorption systems and it is therefore necessary to optimize the variables of time and in these connections, three kinetic models, namely Lagergren-first-order, pseudo-second-order, and intraparticle diffusion equations, have been applied.

3.3.1. Pseudo-first-order Lagergren equation

The model is based on the assumption that adsorption of an ion onto the adsorbent surface is reversible and followed first-order kinetics. The hypothetical reaction may be expressed as:

$$B \underset{k_d}{\overset{k_a}{\rightleftharpoons}} C$$

where k_a and k_d are the adsorption and desorption rate constants, respectively.

Pseudo-first-order Lagergren's equation may be applied to correlate kinetic adsorption data of systems

nearing equilibrium [50,51]. In order to interpret the results of present study, the following basic Lagergren's equation was used.

$$q_t = q_e(1 - e^{-kt}) \tag{2}$$

By solving the above equation, the values of the rate constant of the reaction were obtained as:

$$\frac{q_t}{q_e} = (1 - e^{-kt})$$

$$e^{-kt} = 1 - \frac{q_t}{q_e}$$

$$-kt = \ln\left(1 - \frac{q_t}{q_e}\right)$$

Linear form of the Lagergren's first-order rate expression is given as:

$$\ln(q_e - q_t) = \ln q_{lm} - kt \tag{3}$$

where q_t is the adsorption capacity (mg/g) at different intervals of time t, q_e is the adsorption capacity (mg/g) at equilibrium, k is the rate constant (min^{-1}) of the reaction, q_{lm} is the Lagergren's maximum adsorption capacity (mg/g).

The results are graphically shown in Fig. 5(A), the rate constants k and q_{lm} were obtained by linear plots of ln (q_e−q_t) against time t, and are reported in Table 3. R^2 value (0.970) obtained indicates that the trimetal-oxide adsorbent successfully follows the Lagergren's first-order kinetic model.

3.3.2. The pseudo-second-order Kinetic model equation

The experimental data was further evaluated based on the pseudo-second-order kinetic model which is usually expressed by the following equation [52]

$$\frac{t}{q_t} = \frac{1}{k_2.q_e} + \frac{t}{q_e}$$

$$\frac{t}{q_t} = \frac{1}{h} + \frac{t}{q_e} \tag{4}$$

where $h = k_2 q_e$ can be described as the initial rate constant as t approaches to zero. q_t is the amount of F^- (mg/g) adsorbed at equilibrium, k_2 is the pseudo-second-order rate constant (g/mg.min). If the pseudo-second-order kinetics is applicable, the plot of t/q_t vs. t will give a linear plot, which would allow the computation of q_e, and k_2, and then the adsorption process may be described as chemisorptions [52].

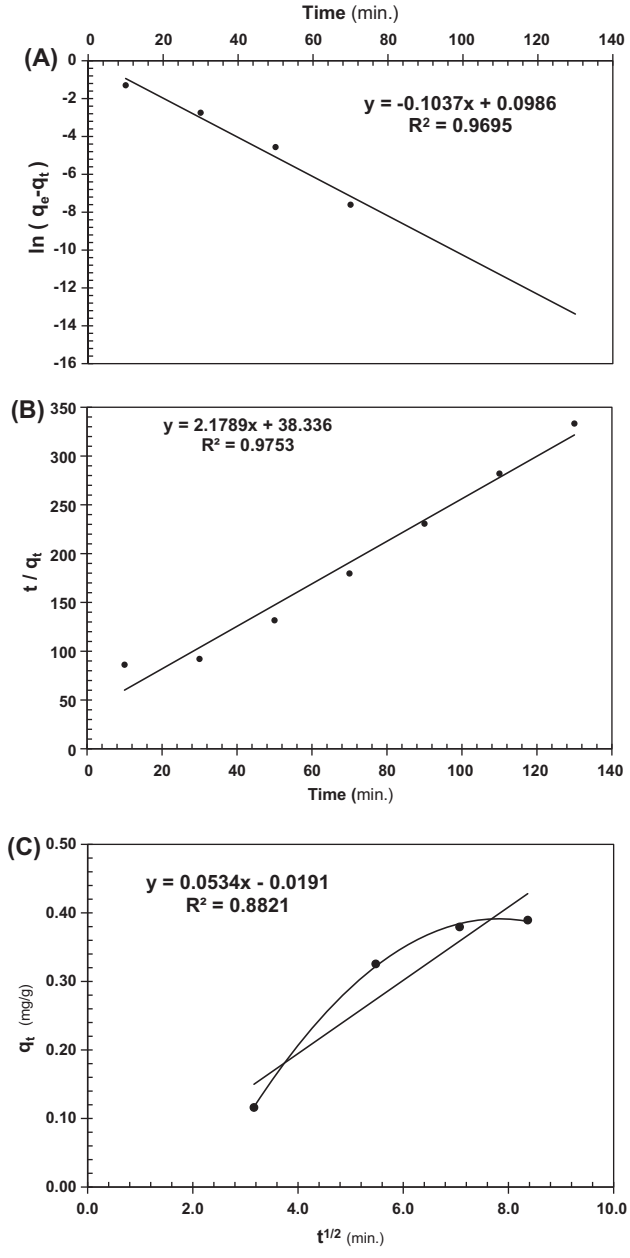

Fig. 5. (A) Plot of Lagergren pseudo-first-order, (B) pseudo-second-order, and (C) intra-particle diffusion model (adsorbent dose = 1 g, initial F^- conc. = 10 mg/L, contact time = 70 min, pH = 7, particle size = 250 μm, shaking speed = 100 rpm).

The experimental data obtained through the study has been fitted into the equation, and a plot of t/q_t vs. t shows a linear relationship (Fig. 5(B)). The adsorption capacity of the adsorbent at equilibrium (q_e), the

Table 3
Adsorption kinetic parameters associated to the Lagergren pseudo-first-order, pseudo-second-order, and intra-particle diffusion models (initial fluoride concentration = 10 mg/L, adsorbent dose = 1 g, volume of adsorbate = 50 mL, pH = 7, shaking speed 100 rpm)

Parameters	Values
Lagergren pseudo-first-order	
R^2	0.970
k (min^{-1})	0.104
q_{lm} (mg/g)	1.104
Pseudo-second-order	
R^2	0.980
k_2 (g/mg min)	0.057
q_e (mg/g)	0.459
Intra-particle diffusion	
R^2	0.808
k_{id}	0.053
C_{id}	0.019

pseudo-second-order rate constant (k_2), and the coefficient of the determination (R^2) have also been evaluated (Table 3). Value of R^2 was found to be 0.980 which indicates that the adsorption process of F^- onto the trimetal-oxide adsorbent follows chemisorption and, therefore, this particular adsorbent is an excellent material for the removal of fluoride ion from aqueous solution.

3.3.3. The intra-particle diffusion equation

The adsorption process on a porous adsorbent generally involves three stages, external diffusion, internal diffusion (or intra-particle diffusion), and actual adsorption. To provide definite information on the rate-limiting step, an internal diffusion model based on Fick's second law is used to test whether the internal diffusion step is the rate-limiting step,

$$qt = k_{id}\, t^{1/2} + C_{id} \tag{5}$$

where k_{id} = internal diffusion constant [mg/(g $min^{1/2}$)].

In order to show the existence of intra-particle diffusion in the adsorption process, the amount of F^- adsorbed (q_t) at different time (t) intervals (10–170 min) was plotted against the square root of time ($t^{1/2}$). The k_{id} and C_{id} values were obtained from the slope and the intercepts of the linear portions of the curves (Table 3). It is seen from Fig. 5(C) that the entire plot has the same general features i.e. the initial curved portion and a linear portion. The initial curved portion is attributed to the boundary layer diffusion, while the linear portion is caused by the intra-particle diffusion [53–56]. The linear portions of the curves do not pass through the origin in Fig. 5(C) and, therefore, indicate that the mechanism of fluoride removal on trimetal-oxide is complex and both the surface adsorption as well as intra-particle diffusion may contribute to the rate determining step.

3.4. Adsorption isotherms

Equilibrium studies between adsorbent and adsorbate are well denoted by adsorption isotherms which are usually the ratio between the quantity of adsorbate adsorbed and its residual amount remaining in solution at certain temperature. Freundlich and Langmuir isotherms are the primitive and the simplest relationships describing the adsorption process [57,58]. These two, the Dubinin–Radushkevich, and Temkin isotherms models have been used for this study to assess the different isotherms and their ability to correlate experimental data.

3.4.1. Langmuir adsorption isotherm

The following linear form of Langmuir equation has been used for the estimation of maximum adsorption capacity corresponding to complete monolayer coverage on surface of this particular adsorbent:

$$\frac{C_t}{q_e} = \frac{1}{kq_{max}} + \frac{C_t}{q_{max}} \tag{6}$$

It is well known that the Langmuir equation is designed for a homogeneous surface and reflects monolayer coverage [59]. The experimental data have been fitted in the above equation by plotting C_t/q_e against C_t (Fig. 6(A)). The q_{max} and k have been determined from the slope and intercept, respectively, with coefficient of determination (R^2) (Table 4). Fig. 6(A) shows a linear plot (R^2 = 0.994) which has been found to be in good agreement with Langmuir adsorption model.

The essential characteristics of the Langmuir isotherm can be expressed in terms of a dimensionless constant separation factor or equilibrium parameter (R_L), which is defined as:

$$R_L = \frac{1}{(1 + b.C_i)} \tag{7}$$

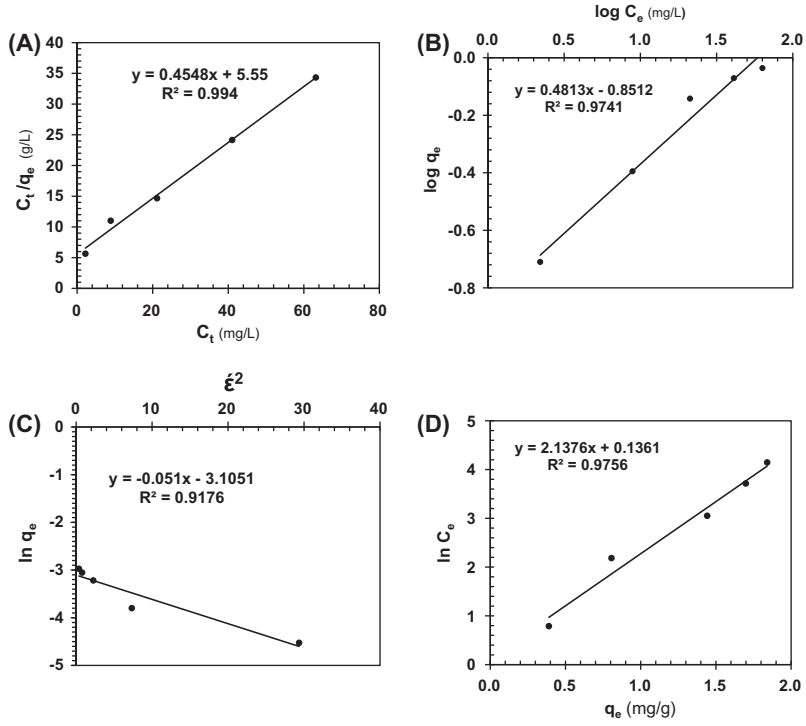

Fig. 6. Plots of (A) Langmuir adsorption isotherm, (B) Freundlich adsorption isotherm, (C) DR isotherm, and (D) Temkin isotherm (adsorbent dose = 1 g, contact time =70 min, pH = 7, particle size = 250 μm, shaking speed = 100 rpm).

Table 4
Langmuir, Freundlich, Dubinin–Radushkevich, and Temkin isotherms constants for the adsorption of fluoride ion on trimetal-oxide adsorbent.

Parameters	Values
Langmuir constants	
R^2	0.994
k	12.203
q_{max}	2.199
R_L	0.005–0.043
Freundlich constants	
R^2	0.974
k	0.141
n	2.078
$1/n$	0.481
DR equation constants	
R^2	0.918
β_D	0.051
q_m	0.045
E (J/mol)	10.10
Temkin constants	
R^2	0.976
β_T	2.138
k_T (L/mg)	1.066

where $b = q_{max}$ is the Langmuir constant and C_i is the initial concentration of F^-.

R_L value indicates the shape of Langmuir isotherm whether adsorption is favorable ($0 < R_L < 1$) or unfavorable ($R_L > 1$), or linear ($R_L = 1$) or irreversible ($R_L = 0$) [49]. The value of R_L has been found to be in the range of $0 < R_L < 1$ (0.005–0.043) and it indicates that the adsorption of fluoride is fairly favorable on the surface of the adsorbent (Table 4).

3.4.2. Freundlich adsorption isotherm

The Freundlich Isotherm model has also been used to estimate the adsorption intensity of the adsorbate toward the adsorbent. The Freundlich adsorption isotherm is mathematically expressed as follows [60]

$$\frac{x}{m} = kC_i^{\frac{1}{n}}$$

$$q = kC_i^{\frac{1}{n}} \tag{8}$$

where k and n are the Freundlich empirical constants [59]. The linearized form of the Freundlich equation is given as:

$$\log q = \log k + \frac{1}{n}\log C_i \tag{9}$$

where C_i (mg/L) and q (mg/g) are the equilibrium liquid phase and equilibrium solid phase ionic concentrations, respectively. Application of the Freundlich equation to analyze the equilibrium isotherm of the fluoride ion onto this particular adsorbent provide a linear plot, and the value of the linear regression co-efficient (R^2) was found to be 0.947, indicating that the data fairly fit in the model.

The values of k and n have been calculated from the slope of Fig. 6(B) and have been found to be 0.141 and 2.078, respectively (Table 4). The calculated k and n values further indicate that the adsorption capacity is quite good and much more favorable for the adsorption of the fluoride onto the trimetal-oxide adsorbent [61,62].

The value of $1/n$ less than unity has been obtained, being an indication that significant adsorption takes place at lower concentration but the increase in the amount adsorbed becomes less significant at higher concentrations and vice versa [59].

3.4.3. Dubinin–Radushkevich isotherm (DR equation)

In order to study the adsorption mechanism, equilibrium data were applied on DR equation [61–63] and is represented by the following equation:

$$q_e = q_m \exp\left[-\beta_D\{\mathrm{RT}\ \ln(1+1/C_e)\}^2\right] \tag{10}$$

The linear form of above equation is given as:

$$\ln q_e = \ln q_m\ - \beta_D\{\mathrm{RT}\ \ln(1+1/C_e)\}]^2 \tag{11}$$

where β_D is related to the free energy of adsorption per mole of the adsorbate as it migrates to the surface of the adsorbent from infinite distance in the solution and q_m is the Dubinin–Radushkevich constant related to the degree of adsorption of adsorbate by the adsorbent [64].

$$\ln q_e = \ln q_m - \beta_D \acute{\varepsilon}^2 \tag{12}$$

Here (Polanyi potential) $\acute{\varepsilon} = \mathrm{RT}\ln(1+1/C_e)$.

A plot of ln q_e against $\acute{\varepsilon}^2$ (Fig. 6(C)) for the trimetal-oxide adsorbent is a straight line, indicating a good fit of the isotherm to the experimental data. The apparent energy (E) of adsorption from Dubinin–Radushkevich isotherm model may be computed using the relationship given below [64].

$$E = \frac{1}{(2\beta_D)^{-\frac{1}{2}}} \tag{13}$$

The mean free energy of adsorption (E) may be calculated from the β_D value using the above equation [65].

The values of DR constants and R^2 values for Dubinin–Radushkevich model are shown in Table 4. The data further indicate that this isotherm also provides very good description of the adsorption process over a range of concentration. The higher values of q_m show high adsorption capacity, whereas if the magnitude of apparent energy of adsorption E is between 8 and 16 kJ/mol, then the adsorption type may be classified as chemisorptions [65]. The E value has been calculated as 10.10 J/mol (Table 4) which also signifies that the adsorption process is chemisorption.

3.4.4. Temkin adsorption isotherm

Temkin adsorption isotherm model is used to evaluate the adsorption potentials of the adsorbent for the adsorbate, and it elaborates that the heat of adsorption of all the molecules in the layer decreases linearly with the coverage due to adsorbate/adsorbent interactions [66–68]. The Temkin isotherm equation is given as:

$$q_e = \beta_T \ln k_T + \beta_T \ln C_e \tag{14}$$

Here, $\beta_T = R_T/b$ is a Temkin isotherm factor related to the heat of the adsorption, whereas K_T is the equilibrium binding constant (L/mg) corresponding to maximum binding energy. Both these constants have been calculated from the slope and intercept of the plot of q_e vs. ln C_e (Fig. 6(D)). The R^2 value has been found to be 0.967 (Table 4) which shows the applicability of the Temkin model for adsorption of fluoride ion onto the trimetal-oxide adsorbent.

4. Conclusion

It has been concluded from the study that the optimum defluoridation efficiency of trimetal-oxide adsorbent (78%) has been achieved between 6.0 and 7.0 at ambient temperature and the removal efficiency increases with the increase in the amount of the adsorbent. A study of different adsorption models indicates that the Langmuir, Freundlich, Dubinin–Radushkevich (DR), and Temkin isotherms may adequately fit the adsorption data and further that pseudo-first-order and pseudo-second-order models are applicable for the whole range of contact time. The adsorbent have also been characterized by WD-XRF and XRD techniques, and the most dominant components have been found to be Al_2O_3, CaO, and MgO with diaspore, calcite, and dolomite being the major minerals phases.

The results obtained fairly substantiate the fact that trimetal-oxide is an excellent adsorbent for the removal of fluoride and may be used as a cheaper alternative for the removal of fluoride ion from aqueous solutions, especially from the groundwater of the Thar Desert of Pakistan.

Acknowledgment

The authors are highly thankful to Pakistan Science Foundation for financial support of this research under Project No. PSF/RES/ S-PCSIR/Env(86).

References

[1] C. Reimann, K. Bjorvatn, B.R. Frengstad, Z. Melaku, R. Tekle-Haimanot, U. Siewers, Drinking water quality in the Ethiopian section of the East African Rift Valley I—data and health aspects, Sci. Total Environ. 311(1–3) (2003) 65–80.

[2] C. Zhu, G. Bai, X. Liu, Y. Li, Screening high-fluoride and high-arsenic drinking waters and surveying endemic fluorosis and arsenism in Shaanxi province in western China, Water Res. 40(16) (2006) 3015–3022.

[3] S. Naseem, T. Rafique, E. Bashir, M.I. Bhanger, A. Laghari, T.H. Usmani, Lithological influences on occurrence of high-fluoride groundwater in Nagar Parkar area, Thar Desert, Pakistan, Chemosphere 78 (11) (2010) 1313–1321.

[4] T. Rafique, S. Naseem, M.I. Bhanger, T.H. Usmani, Fluoride ion contamination in the groundwater of Mithi sub-district, the Thar Desert, Pakistan, Environ. Geol. 56(2) (2008) 317–326.

[5] T. Rafique, S. Naseem, T.H. Usmani, E. Bashir, F.A. Khan, M.I. Bhanger, Geochemical factors controlling the occurrence of high fluoride groundwater in the Nagar Parkar area, Sindh, Pakistan, J. Hazard. Mater. 171(1–3) (2009) 424–430.

[6] T. Rafique, S. Naseem, T.H. Usmani, M.I. Bhanger, K. Shirin, Impact of seawater on distribution of fluoride and other ions in groundwater of Diplo area, Thar Desert Pakistan, Water Environ. Res. 85(7) (2013) 579–586.

[7] US EPA, National Primary Drinking Water Standards, Office of Water EPA 816-F-03-016, 2003. Available at: http://water.epa.gov/safewater.

[8] World Health Organisation, Guidelines for Drinking Water Quality, vol. 1 recommendations, World Health Organization, Geneva, 2004.

[9] S. Ayoob, A.K. Gupta, Fluoride in drinking water: A review on the status and stress effects, Crit. Rev. Environ. Sci. Technol. 36(6) (2006) 433–487.

[10] A. Bhatnagar, E. Kumar, M. Sillanpää, Fluoride removal from water by adsorption: A review, Chem. Eng. J. 171(3) (2011) 811–840.

[11] A.M. Raichur, M. Jyoti Basu, Adsorption of fluoride onto mixed rare earth oxides, Sep. Purif. Technol. 24 (1–2) (2001) 121–127.

[12] V. Tomar, D. Kumar, A critical study on efficiency of different materials for fluoride removal from aqueous media, Chem. Cent. J. 7(1) (2013) 1–15.

[13] S. George, P. Pandit, A.B. Gupta, Residual aluminium in water defluoridated using activated alumina adsorption-modeling and simulation studies, Water Res. 44(10) (2010) 3055–3064.

[14] C. Castel, M. Schweizer, M.O. Simonnot, M. Sardin, Selective removal of fluoride ions by a two-way ion-exchange cyclic process, Chem. Eng. Sci. 55(17) (2000) 3341–3352.

[15] E.J. Reardon, Y. Wang, A limestone reactor for fluoride removal from wastewaters, Environ. Sci. Technol. 34(15) (2000) 3247–3253.

[16] P.L. Bishop, G. Sansoucy, Fluoride removal from drinking water by fluidized activated alumina adsorption, J. Am. Water Works Assoc. 70(10) (1978) 554–559.

[17] M. Hichour, F.O. Persin, J. Sandeaux, C. Gavach, Fluoride removal from waters by Donnan dialysis, Sep. Purif. Technol. 18(1) (1999) 1–11.

[18] Z. Amor, B. Bariou, N. Mameri, M. Taky, S. Nicolas, A. Elmidaoui, Fluoride removal from brackish water by electrodialysis, Desalination 133(3) (2001) 215–223.

[19] F. Durmaz, H. Kara, Y. Cengeloglu, M. Ersoz, Fluoride removal by donnan dialysis with anion exchange membranes, Desalination 177(1–3) (2005) 51–57.

[20] K. Hu, J.M. Dickson, Nanofiltration membrane performance on fluoride removal from water, J. Membr. Sci. 279(1–2) (2006) 529–538.

[21] M.S. Onyango, H. Matsuda, Fluoride removal from water using adsorption technique, Adv. Fluorine Sci. 2 (2006) 1–48.

[22] A. Tor, Removal of fluoride from an aqueous solution by using montmorillonite, Desalination 201(1–3) (2006) 267–276.

[23] Y.-H. Li, S. Wang, A. Cao, D. Zhao, X. Zhang, C. Xu, Z. Luan, D. Ruan, J. Liang, D. Wu, Adsorption of fluoride from water by amorphous alumina supported on carbon nanotubes, Chem. Phys. Lett. 350(5–6) (2001) 412–416.

[24] R. Lavecchia, F. Medici, L. Piga, G. Rinaldi, A. Zuorro, Fluoride removal from water by adsorption on a high alumina content bauxite, Chem. Eng. 26 (2012) 225–230.

[25] W. Li, C.-Y. Cao, L.-Y. Wu, M.-F. Ge, W.-G. Song, Superb fluoride and arsenic removal performance of highly ordered mesoporous aluminas, J. Hazard. Mater. 198 (2011) 143–150.

[26] Y. Ku, H.-M. Chiou, The adsorption of fluoride ion from aqueous solution by activated alumina, Water Air Soil Pollut. 133(1/4) (2002) 349–361.

[27] A.K. Chaturvedi, K.P. Yadava, K.C. Pathak, V.N. Singh, Defluoridation of water by adsorption on fly ash, Water Air Soil Pollut. 49(1–2) (1990) 51–61.

[28] W. Rongshu, L. Haiming, N. Ping, W. Ying, Study of a new adsorbent for fluoride removal from waters, Water Q. Res. J. Can. 30(1) (1995) 81–88.

[29] D.S. Bhargava, D.J. Killedar, Fluoride adsorption on fishbone charcoal through a moving media adsorber, Water Res. 26(6) (1992) 781–788.

[30] M.S. Onyango, Y. Kojima, O. Aoyi, E.C. Bernardo, H. Matsuda, Adsorption equilibrium modeling and solution chemistry dependence of fluoride removal from water by trivalent-cation-exchanged zeolite F-9, J. Colloid Interface Sci. 279(2) (2004) 341–350.

[31] X. Yu, S. Tong, M. Ge, J. Zuo, Removal of fluoride from drinking water by cellulose@ hydroxyapatite nanocomposites, Carbohydr. Polym. 92(1) (2013) 269–275.

[32] S.K. Swain, T. Patnaik, R.K. Dey, Efficient removal of fluoride using new composite material of biopolymer alginate entrapped mixed metal oxide nanomaterials, Desalin. Water Treat. 51(22–24) (2013) 4368–4378.
[33] W.-Y. Li, J. Liu, H. Chen, Y. Deng, B. Zhang, Z. Wang, X. Zhang, S. Hong, Application of oxalic acid cross-linking activated alumina/chitosan biocomposites in defluoridation from aqueous solution. Investigation of adsorption mechanism, Chem. Eng. J. 225 (2013) 865–872.
[34] S.K. Swain, T. Patnaik, P.C. Patnaik, U. Jha, R.K. Dey, Development of new alginate entrapped Fe(III)–Zr(IV) binary mixed oxide for removal of fluoride from water bodies, Chem. Eng. J. 215–216 (2013) 763–771.
[35] J. Wang, W. Xu, L. Chen, Y. Jia, L. Wang, X.-J. Huang, J. Liu, Excellent fluoride removal performance by CeO_2–ZrO_2 nanocages in water environment, Chem. Eng. J. 231 (2013) 198–205.
[36] S. Deng, H. Liu, W. Zhou, J. Huang, G. Yu, Mn–Ce oxide as a high-capacity adsorbent for fluoride removal from water, J. Hazard. Mater. 186(2–3) (2011) 1360–1366.
[37] X. Dou, Y. Zhang, H. Wang, T. Wang, Y. Wang, Performance of granular zirconium-iron oxide in the removal of fluoride from drinking water, Water Res. 45(12) (2011) 3571–3578.
[38] R. Jha, U. Jha, R.K. Dey, S. Mishra, S.K. Swain, Fluoride sorption by zirconium (IV) loaded carboxylated orange peel, Desalin. Water Treat. (2013) 1–14. http://dx.doi.org/10.1080/19443994.2013.862742.
[39] D. Mohan, R. Sharma, V.K. Singh, P. Steele, C.U. Pittman Jr., Fluoride removal from water using biochar, a green waste, low-cost adsorbent: Equilibrium uptake and sorption dynamics modeling, Ind. Eng. Chem. Res. 51(2) (2012) 900–914.
[40] V. Hernández-Montoya, L.A. Ramírez-Montoya, A. Bonilla-Petriciolet, M.A. Montes-Morán, Optimizing the removal of fluoride from water using new carbons obtained by modification of nut shell with a calcium solution from egg shell, Biochem. Eng. J. 62 (2012) 1–7.
[41] V. Ganvir, K. Das, Removal of fluoride from drinking water using aluminum hydroxide coated rice husk ash, J. Hazard. Mater. 185(2–3) (2011) 1287–1294.
[42] H. Yoshitake, T. Yokoi, T. Tatsumi, Adsorption of chromate and arsenate by amino-functionalized MCM-41 and SBA-1, Chem. Mater. 14(11) (2002) 4603–4610.
[43] P.L. Bailey, Analysis with Ion-selective Electrodes, Heyden, London, 1980.
[44] R. Leyva-Ramos, N.A. Medellin-Castillo, A. Jacobo-Azuara, J. Mendoza-Barron, L.E. Landin-Rodriguez, J.M. Martinez-Rosales, A. Aragon-PiãA, Fluoride removal from water solution by adsorption on activated alumina prepared from pseudo-boehmite, J. Environ. Eng. Manage. 18(5) (2008) 301–309.
[45] G. Karthikeyan, N.M. Andal, K. Anbalagan, Adsorption studies of iron(III) on chitin, J. Chem. Sci. 117(6) (2005) 663–672.
[46] S.A. Khan, M.A. Riaz-ur-Rehman, Sorption of cobalt on bentonite, J. Radioanal. Nucl. Chem. 207(1) (1996) 19–37.
[47] Z. Aksu, U. Açikel, E. Kabasakal, S. Tezer, Equilibrium modelling of individual and simultaneous biosorption of chromium(VI) and nickel(II) onto dried activated sludge, Water Res. 36(12) (2002) 3063–3073.
[48] J. Rouquerol, D. Avnir, C.W. Fairbridge, D.H. Everett, J.M. Haynes, N. Pernicone, J.D.F. Ramsay, K.S.W. Sing, K.K. Unger, Recommendations for the characterization of porous solids (technical report), Pure Appl. Chem. 66(8) (1994) 1739–1758.
[49] S. Meenakshi, A. Pius, G. Karthikeyan, B.V.A. Rao, The pH dependence of efficiency of activated alumina in defluoridation of water, Indian J. Environ. Prot. 11 (1991) 511–513.
[50] S. Lagergren, Zur theorie der sogenannten adsorption geloster stoffe (About the theory of so-called adsorption of soluble substances), Kungliga svenska vetenskapsakademiens handlingar, 24(4) (1898) 1–39.
[51] S. Rengaraj, C.K. Joo, Y. Kim, J. Yi, Kinetics of removal of chromium from water and electronic process wastewater by ion exchange resins: 1200H, 1500H and IRN97H, J. Hazard. Mater. 102(2–3) (2003) 257–275.
[52] Y.S. Ho, D.A. John Wase, Batch nickel removal from aqueous solution by sphagnum moss peat, Water Res. 29(5) (1995) 1327–1332.
[53] G.S. Gupta, G. Prasad, K.K. Panday, V.N. Singh, Removal of chrome dye from aqueous solutions by fly ash, Water Air Soil Pollut. 37(1–2) (1988) 13–24.
[54] C. Namasivayam, R.T. Yamuna, Adsorption of direct red 12 B by biogas residual slurry: Equilibrium and rate processes, Environ. Pollut. 89(1) (1995) 1–7.
[55] R. Qadeer, J. Hanif, Adsorption of uranium in the presence of different cations on activated-charcoal, J. Chem. Soc. Pak. 15(4) (1993) 227–230.
[56] R. Qadeer, J. Hanif, M. Khan, M. Saleem, Uptake of uranium ions by molecular sieve, Radiochim. Acta 68 (1995) 197–202.
[57] N. Muhammad, J. Parr, M.D. Smith, A.D. Wheatley, Adsorption of heavy metals in slow sand filters, 24 (1998) 346–349.
[58] R. Jalali, H. Ghafourian, Y. Asef, S.J. Davarpanah, S. Sepehr, Removal and recovery of lead using nonliving biomass of marine algae, J. Hazard. Mater. 92(3) (2002) 253–262.
[59] H. Teng, C.-T. Hsieh, Influence of surface characteristics on liquid-phase adsorption of phenol by activated carbons prepared from bituminous coal, Ind. Eng. Chem. Res. 37(9) (1998) 3618–3624.
[60] H. Freundlich, Ueber die adsorption in loesungen Zeitschrift fr Physikalische, (Adsorption in solutions), Z. Phys. Chem. 57A (1907) 385–470.
[61] A. Akgerman, M. Zardkoohi, Adsorption of phenolic compounds on fly ash, J. Chem. Eng. Data 41(2) (1996) 185–187.
[62] K. Kadirvelu, C. Namasivayam, Agricultural by-product as metal adsorbent: Sorption of lead(II) from aqueous solution onto coirpith carbon, Environ. Technol. 21(10) (2000) 1091–1097.
[63] M. Mahramanlioglu, I. Kizilcikli, I.O. Bicer, Adsorption of fluoride from aqueous solution by acid treated spent bleaching earth, J. Fluorine Chem. 115(1) (2002) 41–47.
[64] M. Horsfall, A.I. Spiff, A.A. Abia, Studies on the influence of mercaptoacetic acid (maa) modification of cassava (manihot sculenta cranz) waste biomass on the adsorption of Cu^{2+} and Cd^{2+} from aqueous solution, Bull. Korean Chem. Soc. 25(7) (2004) 969–976.

[65] S.H. Chien, W.R. Clayton, Application of Elovich Equation to the kinetics of phosphate release and sorption in soils, Soil Sci. Soc. Am. J. 44(2) (1980) 265–268.
[66] R.R. Sheha, E. Metwally, Equilibrium isotherm modeling of cesium adsorption onto magnetic materials, J. Hazard. Mater. 143(1–2) (2007) 354–361.
[67] I.B. Solangi, S. Memon, M.I. Bhanger, An excellent fluoride sorption behavior of modified amberlite resin, J. Hazard. Mater. 176(1–3) (2010) 186–192.
[68] J. Anwar, U. Shafique, M. Salman, S. Waheed-uz-Zaman, S. Anwar, Removal of chromium (III) by using coal as adsorbent, J. Hazard. Mater. 171(1–3) (2009) 797–801.